ARID ZONE JOURNAL OF ENGINEERING, TECHNOLOGY & ENVIRONMENT
AZOJETE March 2026. Vol.22(1):137-148
Published by the Faculty of Engineering, University of Maiduguri, Maiduguri, Nigeria.
Print ISSN: 1596-2490, Electronic ISSN: 2545-5818
https://doi.org/10.63958/AZOJETE/2026/22/01/012
www.azojete.com.ng

DEVELOPMENT

DESIGN, CONSTRUCTION, AND CALIBRATION OF A LOW-COST PORTABLE DIP-COATING MACHINE FOR LABORATORY APPLICATIONS

M. A. Abdulrahman[1,3]*, M. Sumaila[1], M. Dauda[1], O. K. Abubakre[2,3]

[1] *Department of Mechanical engineering Ahmadu Bello University Zaria, Nigeria*
[2] *Department of Materials and Metallurgical Engineering, Federal University of Technology Minna, Nigeria*
[3] *Centre of Genetics Engineering and Biotechnology, Federal University of Technology Minna, Nigeria*
Corresponding author's email: send2mahmudmalik@yahoo.com

ARTICLE INFORMATION

Received: 27th December 2025
Revised: 3rd February 2026
Accepted: 3rd February 2026

Keywords:
Dip-coater
Calibration
Arduino-uno
Immersion height
Withdrawal speed
Potentiometer
NEMA 17 stepper motor

ABSTRACT

Precise control of withdrawal speed and immersion height is essential for achieving uniform coatings and ensuring process reproducibility in dip-coating techniques. Commercial dip-coating systems capable of such control are often costly, limiting their accessibility to emerging and resource-constrained laboratories. This work reports the design, fabrication, and performance evaluation of a simple, portable, and low-cost automated dip-coating system intended for laboratory-scale surface coating applications. The system integrates mechanical and electronic subsystems, with the motor–lead screw assembly selected based on fundamental mechanical design principles. Automated control of immersion and withdrawal processes was implemented using an Arduino Uno microcontroller. Calibration of immersion height and withdrawal speed was performed using a Vernier caliper and a tachometer, respectively. The assembled system demonstrated reliable operation within an immersion height range of 70–220 mm and a withdrawal speed range of 0.5–7 mm s^{-1}, with maximum deviations of 0.75% and 2.0%, respectively. The total material cost of the dip coater was approximately USD 97. The adjustable immersion height feature enables reduced operational time and improved energy efficiency during coating processes. Owing to its accuracy, reproducibility, and affordability, the developed system offers a practical alternative to commercial dip coaters for thin-film deposition and surface protection research.

1.0 Introduction

Dip coating is a versatile, scalable, and cost-effective technique for depositing thin films on a wide range of substrates. The process involves immersing a substrate into a solution or suspension, allowing sufficient wetting and interfacial interaction, followed by withdrawal at a controlled and constant speed. During withdrawal, a liquid film is entrained on the substrate surface and subsequently solidifies through solvent evaporation or curing, resulting in coatings with well-defined thickness and properties (Tang and Yan, 2017; Nguyen *et al.,* 2018). Owing to its simplicity, compatibility with diverse material systems, and ease of scale-up, dip coating has been widely adopted in both academic research and industrial manufacturing. Applications include ferroelectric and dielectric devices, sensors and actuators, membranes, superconducting layers, protective coatings, and passivation layers (Anwar *et al.,* 2017; Brinker, 2013). The quality, uniformity, and functional performance of dip-coated films are governed by several processing parameters, including solution composition, viscosity, density, immersion time, withdrawal speed, number of coating cycles, drying conditions, and substrate surface properties (Ceratti *et al*., 2015). Among these parameters, withdrawal speed plays a dominant role, as it directly controls film thickness and homogeneity through hydrodynamic and evaporation-driven mechanisms (Tang and Yan, 2017). Consequently, precise and reproducible control of withdrawal speed, immersion depth, and residence time is essential for achieving consistent coating quality. Automated dip-coating systems are therefore commonly employed to ensure reliable process control. However, commercial dip coaters are often prohibitively expensive, limiting their accessibility, particularly in newly

established or resource-constrained laboratories. In response to this challenge, increasing attention has been directed toward the development of low-cost, custom-built dip-coating systems based on microcontrollers, stepper motors, and open-source hardware. Several studies have demonstrated the feasibility of such approaches. Adámek (2016) reported a programmable system with withdrawal speeds up to 20 mm s^{-1}. Yahandri *et al.* (2019) developed a microcontroller-based dip coater operating between 0.02 and 10 mms^{-1} with a reported control accuracy of 96.57%. Dunlap *et al.* (2022) and Castillo-Vilcatoma *et al.* (2022) further reduced system cost by employing simplified mechanical designs and repurposed components, achieving stable withdrawal speeds below USD 600 and USD 100, respectively. More recently, Guzman-Valdivia *et al.* (2025) demonstrated an ultra-low-cost, 3D-printed dip-coating system integrated with an Arduino controller and graphical user interface, with a total component cost of approximately USD 50. Serrano-Perez *et al.* (2023) introduced a revolving dip-coating system incorporating PID control, significantly reducing deposition time while maintaining excellent dynamic performance. Despite these advances, many reported low-cost dip coaters suffer from limitations such as restricted withdrawal-speed resolution, mechanical instability at low speeds, reliance on non-standardized or scavenged components, or the capability to process only a single substrate per coating cycle (Adámek 2016; Dunlap *et al.* 2022; Serrano-Perez *et al.* 2023). The lack of multi-sample processing capability is particularly restrictive for systematic materials optimization and statistically robust thin-film studies, especially at very low withdrawal speeds where sequential coating becomes impractically time-consuming. In this work, we present the design and development of a low-cost, portable, microcontroller-based dip-coating system capable of simultaneously processing two or more substrates under identical and precisely controlled coating conditions. A locally developed dipping system supports academic training, enables flexible customization for specific research needs, promotes indigenous technology development, and allows researchers in resource-limited settings to conduct reliable and reproducible thin-film studies without compromising essential performance.

2. Materials and Methods

2.1 Materials

The materials and components used in the design and fabrication of the dip-coating machine include 25mm carbon steel angle section, acrylic sheets, an Acme lead screw, 608 ball and thrust bearings, M6 bolts and nuts, crocodile clips, a PLA 3D-printed carriage, steel guide rods, hinges, steel pipes and plates, a flexible coupling, retaining clips, a NEMA 17 stepper motor, a potentiometer, an LCD display, an Arduino microcontroller, an A4988 stepper motor driver, a keypad, a 12 V power adaptor, an electronic prototyping board, and insulated connecting wires.

2.2 Description of the Dip-Coating Machine

The dip-coating machine developed in this work consists of two main subsystems: (i) the mechanical subsystem and (ii) the electronic control subsystem. A schematic representation of the complete system is shown in Figure 1.

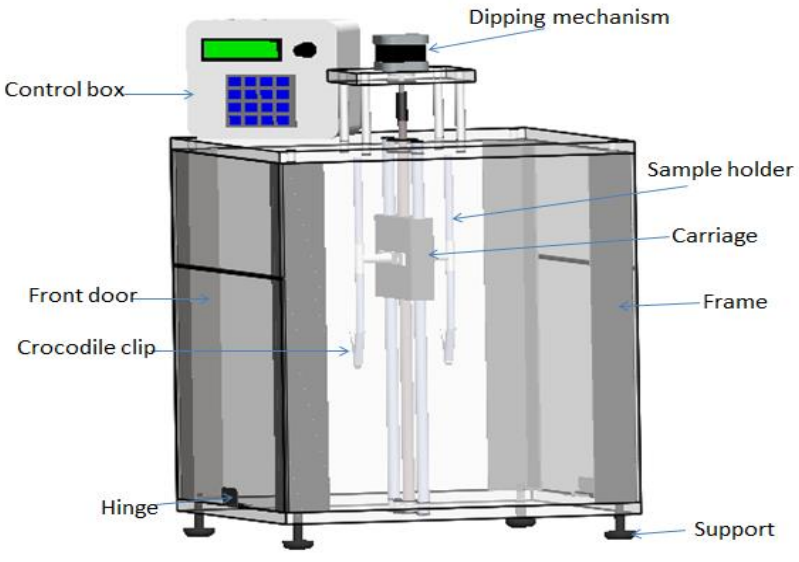

Figure 1: Schematic Drawing of the Dip-Coating Machine

Corresponding author's email address: send2mahmudmalik@yahoo.com

2.2.1 Mechanical subsystem

The mechanical subsystem of the dip-coating machine, illustrated by the isometric view in Figure 1, comprises a rigid support frame and a vertically actuated dipping mechanism. The frame is constructed from carbon steel angle section and acrylic plates, forming a box-like structure that provides both mechanical rigidity and visibility of the coating process. The entire assembly is mounted on four swiveling leveling feet, which ensure stable positioning and allow fine adjustment on uneven laboratory surfaces. The dipping mechanism consists of a vertically moving PLA 3D-printed carriage designed to accommodate multiple sample holders. Each sample holder is fabricated from a hollow steel pipe and fitted with crocodile clips at the lower end to securely grip the substrates during immersion and withdrawal. Vertical motion of the carriage is achieved through an Acme lead screw driven by a stepper motor. The motor shaft is coupled to the lead screw via a flexible coupling, which minimizes misalignment and reduces the transmission of vibrations, thereby enabling smooth and precise linear motion throughout the dip-coating process.

2.2.2 Electronic control subsystem

The electronic control subsystem of the dip-coating machine, shown schematically in Figure 2, comprises an Arduino Uno microcontroller, an A4988 stepper motor driver, a potentiometer for speed adjustment, a keypad for user input, a liquid crystal display (LCD) for parameter visualization, and a 12 V DC power supply.

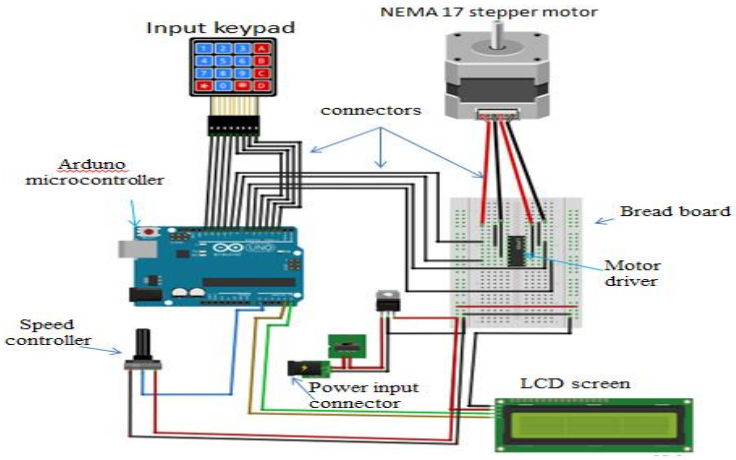

Figure 2: Schematic diagram of the dip-coater electronic circuit

The Arduino Uno serves as the central control unit, executing the programmed control logic and generating step and direction signals for the stepper motor driver. The A4988 motor driver converts these signals into precisely regulated current pulses that drive the stepper motor, enabling accurate control of the carriage displacement and withdrawal speed. The potentiometer allows real-time adjustment of the motor speed, while the keypad facilitates user input of operational parameters such as travel height and residence time. The LCD display provides continuous feedback on system status and process variables. All electronic components are mounted on an electronic circuit board and housed within a perforated polymer enclosure. This enclosure provides electrical insulation and mechanical protection while allowing adequate ventilation to prevent overheating during operation, thereby ensuring safe and reliable performance of the dip-coating machine.

2.3 Dip-Coating Machine Operation

The operational sequence of the dip-coating machine is summarized in the flowchart shown in Figure 3**.** Upon powering the system, the Arduino microcontroller initializes all peripherals and displays the program name on the LCD, indicating system readiness. The user initiates the process by pressing the *Start* button on the keypad. The system then prompts the user to input the immersion distance, followed by the dwelling time, both of which are entered and confirmed using the keypad. Next, the withdrawal speed is set manually via the potentiometer. The user may then adjust the initial height of the sample relative to the coating solution using the height adjustment function, allowing the carriage to be moved upward or downward as required. Once all parameters are configured, pressing the Start button again initiates the automated dip-coating cycle. During operation, the carriage moves downward to immerse the sample into the coating solution by the specified distance, remains stationary for the predefined dwelling time, and is then withdrawn upward at the set speed.

Corresponding author's email address: send2mahmudmalik@yahoo.com

Upon completion of the cycle, the system returns to an idle state, allowing the user either to repeat the coating process with the same parameters or to input new parameters for subsequent cycles.

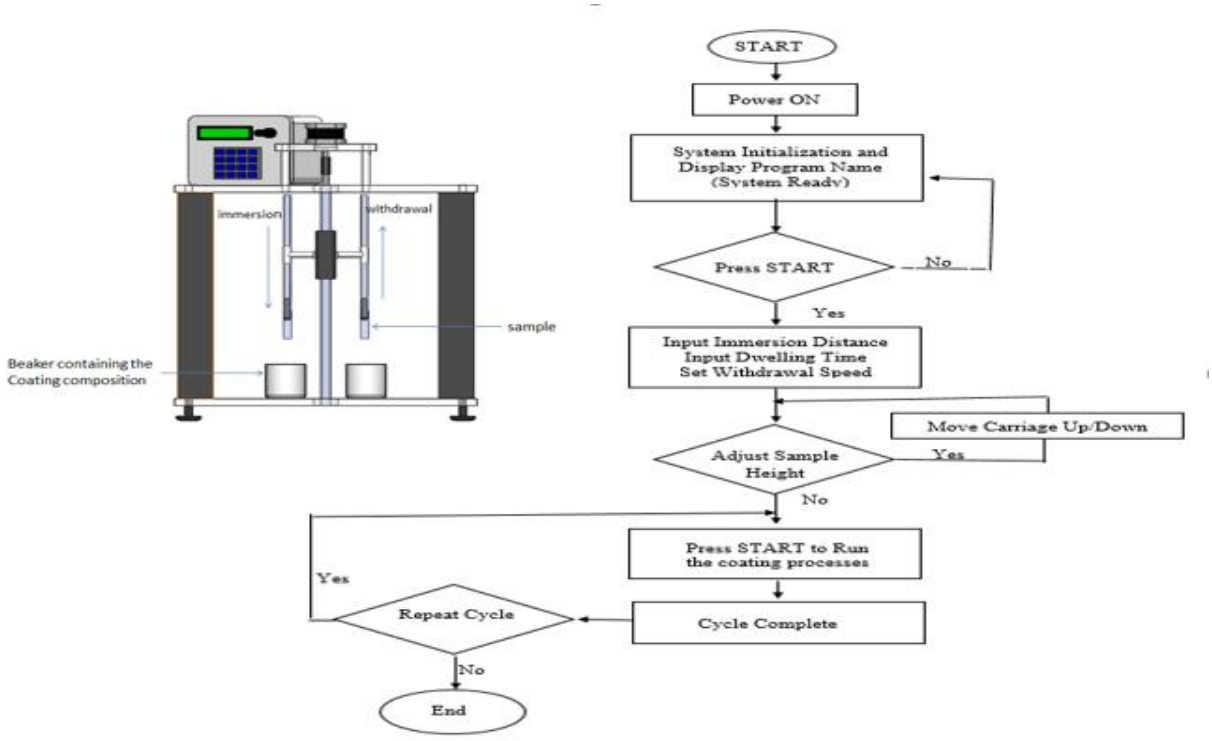

Figure 3: Flowchart of the dip-coating machine operation

2.4 Design Considerations

The dip coater was designed using readily available, low-cost components to achieve a simple, portable, and efficient coating system. The height of a 250ml Pyrex beaker (100mm), a sample length of 100mm with the clearance of 10mm between were considered in designing the maximum carriage travel height of 150 mm from a predefined reference point. The system operates within a controlled withdrawal speed range of 1–7 mm s^{-1} with an adjustable travel height to accommodate varying solution levels and container dimensions. The reference height was made to be adjustable, thereby minimizing unnecessary motion, reducing coating time, and improving energy efficiency. The device was designed to simultaneously coat two samples, each with a maximum mass of 200 g. Control and automation coding was self-developed and implemented using C++ programming. The system allows user-defined input of key process parameters, including immersion height, dwelling time, and withdrawal speed. These parameters are entered via an integrated keypad and displayed on an LCD screen to ensure precise and repeatable operation. The mechanical structure was designed for easy assembly and disassembly, enhancing portability, maintenance, and system flexibility.

2.5 Design Theory

The electric motor and screw rod constitute the core components of the dip coater's linear actuation mechanism. The electric motor provides the driving force required to translate the carriage vertically in accordance with the programmed motion profile. Electric motors are available in various types, sizes, and power ratings; therefore, appropriate motor selection is critical to ensure reliable and efficient operation. The capacity of an electric motor is defined by the torque and speed it can deliver. Consequently, motor selection for the dip coater was based on the evaluation of the minimum required operating torque, which is determined by the total load acting on the system. This load includes the combined weight of the coated samples, the sample holder, the holder support, and the carriage assembly. Accurate estimation of this load ensures that the selected motor can overcome gravitational forces and mechanical losses while maintaining the desired withdrawal and immersion velocities.

The weights of the carriage, sample holder support, sample holder was computed using Equation 1 as given by

$$\rho = \frac{M}{V} \qquad 1$$

Corresponding author's email address: send2mahmudmalik@yahoo.com

Where; ρ = Density of the material, M = Mass of the material, V = Volume of the material.

The carriage (as shown in Figure 4) was made from Polylactic Acid (PLA) with a density of 1250kg/m^3 at 50^{o}C and the sample holder support and the sample holder were made from mild steel pipe with density of 7860kg/m^3.

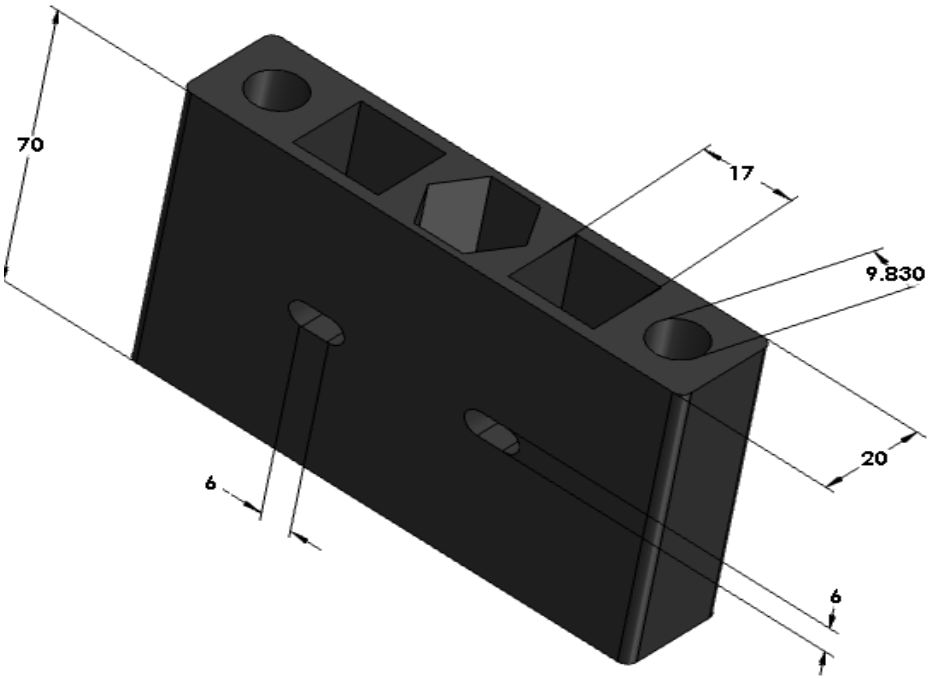

Figure 4: Isometric Drawing of the Carriage

The volume of the carriage was determined from the dimensions of the carriage using Equation 2.

$$V_c = V_s - V_r \quad (2)$$

Where; V_c = Volume of the carriage, V_s = Volume of the solid carriage block and V_r = Total volume of the recesses on the carriage block.

The volume of the solid carriage block was calculated from Equation 3

$$V_s = Length \times width \times breadth \quad (3)$$

The carriage consists of three recesses which are cylindrical, cuboids and slot like. The cylindrical recesses are those through which the plane rod passes, which constraint the carriage to move in the vertical direction, the cuboids recesses are provided for weight reduction, while the slots like recesses were provided for bolting the sample holder support to the carriage. The volume of the cylindrical, cuboid and slots like recesses were evaluated using Equation 5, 6 and 7.

$$V_r = 4V_{rcd} + 2V_{rc} + 2V_{rs} \quad (4)$$

$$V_{rcd} = \frac{\pi d^2 h}{4} \quad (5)$$

$$V_{rc} = L_{rc} \times B_{rc} \times H_{rc} \quad (6)$$

$$V_{rs} = \frac{\pi {d_{rs}}^2 \times L_{rs} \times B_{rs} \times H_{rs}}{4} \quad (7)$$

Where: V_{rcd} = Volume of the cylindrical recesses, V_{rc} = Volume of the cuboid recesses, V_{rs} = Volume of the slot, d = Diameter of the cylindrical slot, h = Height of the carriage, L_{rc} = Length of the cuboid recess, B_{rc} =

Corresponding author's email address: send2mahmudmalik@yahoo.com

Width of cuboid recess, H_{rc} = Height of the cuboid recess, d_{rs} = Diameter of the slot recess, L_{rs} = Length of the slot recess and H_{rs} = width of the carriage.

The carriage was printed with 40% infill; thus, the final volume of the carriage was obtained from Equation 8.

$$V_{fc} = 0.4(V_c) \quad (8)$$

$$V_c = V_s - V_r \quad (9)$$

Where;V_c = Final volume of the carriage, V_{fc} = Final carriage volume at 40% infill,

The sample holder supports were made in form of T-shape with hollow pipe and the base welded to a flat plate. The sample holder supports volume were calculate using Equation 10.

$$V_{shs} = \frac{2(D_{shs}{}^2 - d_{shs}{}^2)L_{shs}}{4} + L_p \times H_p \times t_p \quad (10)$$

Where; V_{shs} = Volume of the sample holder support, D_{shs} = Outer diameter of the pipe, d_{shs} = Inner diameter of the pipe, L_{shs} = Length of the pipe, L_p = Length of the welded plate, H_p = height of the plate, t_p = Thickness of the plate

The sample holders were made from mild steel pipe with crocodile clip screw to the lower end. The volume of the sample holder pipe was determined using Equation 11 and the mass of the crocodile clips were weighed directly.

$$V_{sh} = \frac{2(D_{sh}{}^2 - d_{sh}{}^2)L_{sh}}{4} \quad (11)$$

Where; V_{sh} = Volume of the sample holders, Dsh = Outer diameter of the sample holder, d_{sh} = inner diameter of the sample holder, L_{sh} = Length of the sample holder

The dip coater was design to support two mild steel samples of 200g each. The total weight of the carriage, sample holder support, the sample holders and the samples were evaluated from Equation (12) (Idris *et al.,* 2018).

$$W_T = 9.81(1250(V_{fc}) + 7860(V_{shs} + V_{sh}) + 2M_{ccd} + 2M_s) \quad (12)$$

Where; M_{ccd} = Mass of the crocodile clip, M_s = Mass of samples

The coefficient of friction between PLA and mild steel was taken as 0.3. Therefore, the operating weight, Wo, was computed using Equation 13 as given by Khurmi and Gupta (2005)

$$W_o = 1.667 \times W_T \quad (13)$$

Acme screw thread was used to lift the samples with the help of the carriage. The screw was considered as a power screw and the effort required to lift the load, W_o, was calculated from the Equation 14 as presented by Khurmi and Gupta (2005)

$$P = W_o \tan(\alpha + \varphi) \quad (14)$$

Where; P = Lifting effort, α = Angle inclination, ϕ = Friction angle between the screw and the nut

The torque required to lift the sample from the suspension was obtained using Equation (15) (Khurmi and Gupta 2005);

$$T = \frac{Pd}{2} \quad (15)$$

Where; T = Lifting Torque d = Mean diameter of the screw

Corresponding author's email address: send2mahmudmalik@yahoo.com

The stepper motor used was selected base on the estimated torque from Equation (15).

The screw was considered as a column with both ends fixed and the crippling load for the column was estimated using the Rankine-Gordon formula as given by Equation 16.

$$W_{cr} = A_c \times \sigma_y \left[1 - \frac{\sigma_y}{4C\pi^2 E}\left(\frac{L}{k}\right)^2\right] \quad 16$$

2.6 Design Calculation

Design calculations were performed using standard mechanical design theory (Equations 1–16). The torque required to lift the fully loaded carriage was calculated to be 3.25 Ncm. A readily available NEMA 17 stepper motor with a rated torque of 0.4 Nm was selected, providing a factor of safety of approximately 100, which is significantly greater than the allowable value of 1.5. The lead screw's critical (crippling) load was calculated to be 11.8 kN, which is approximately four orders of magnitude greater than the applied carriage load of 3.898 N. This large margin confirms excellent mechanical stability. These results indicate that the system can reliably support the carriage and maintain smooth and safe operation under all expected operating conditions.

2.7 Construction and Assembly of the Dip Coating Machine

2.7.1 Construction of the machine parts

The major components of the machine namely the machine frame, the coating mechanism, and the machine control unit were fabricated using basic manufacturing techniques such as cutting, drilling, welding, grinding, and soldering

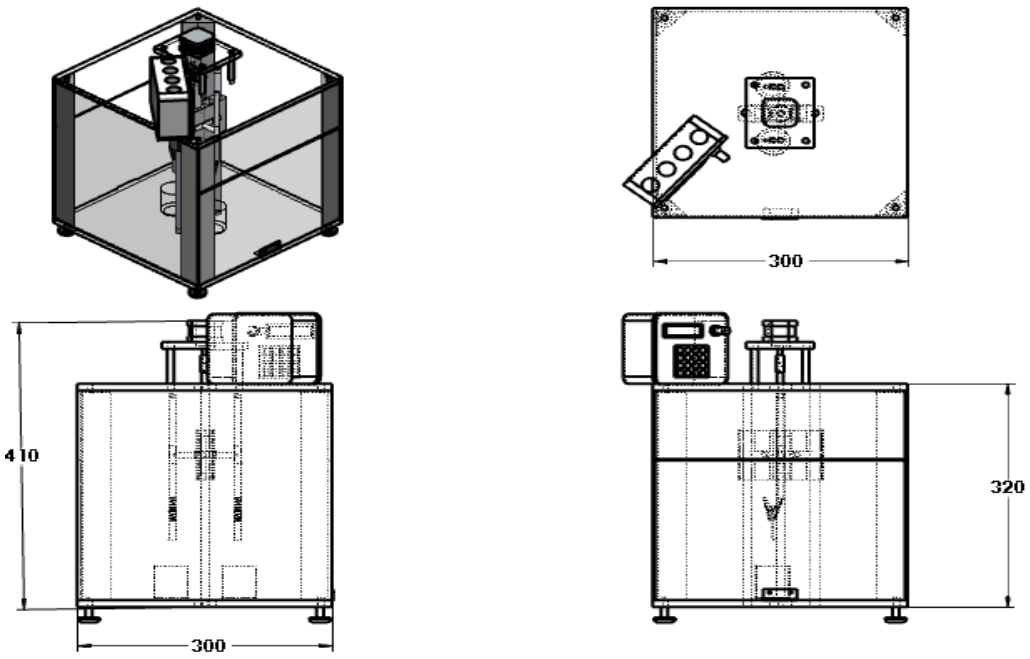

Figure 5: Orthographic Views of the Dip Coating Machine

i. Construction of the machine frame

The dip coater was designed in a box configuration to ensure structural stability and ease of enclosure. The overall frame height of 320 mm (as shown in Figure 5) was selected to accommodate the maximum required dipping depth and vertical travel of the substrate holder. Mild steel angle section of 25×25 mm was chosen to provide sufficient rigidity while keeping the weight of the structure moderate and economical. Acrylic plates were used for the top, base, and side covers due to their light weight, corrosion resistance, transparency, and ease of machining. A thickness of 10 mm was selected for the top and base plates to ensure adequate stiffness under the motor and coating solution's load, while 3 mm thick acrylic was sufficient for the side covers, which do not bear significant loads. The 7 mm holes were drilled to accommodate standard M6 bolts, ensuring ease

Corresponding author's email address: send2mahmudmalik@yahoo.com

of assembly and maintenance. The mounting platform dimensions were selected to match the footprint of the NEMA 17 stepper motor.

Plate I: stages of the construction (a) frame (b) coating chamber, (c) control system and (d) assembled of the dip coating machine

ii. Dipping mechanism

Two plain guide rods, each 340 mm in length and 10 mm in diameter, were used to guide the vertical motion of the sample carriage. The rod length was selected to accommodate the required dipping stroke while providing sufficient clearance above the coating container. A rod diameter of 10 mm was chosen to ensure adequate stiffness and minimize deflection during operation. The sample carriage, measuring 70 × 90 × 22 mm, was designed in SolidWorks 2022 (as show in Figure 4) and fabricated by 3D printing, its dimensions were determined based on the maximum sample size and the need to house the guide rod recesses securely. A 350 mm long Acme lead screw with a nominal diameter of 10 mm was employed to drive the carriage, as Acme threads provide improved load-bearing capacity and reduced backlash for precise vertical motion. Both ends of the screw were turned to 8.5 mm to allow proper seating within standard bearings. Two 608 ball bearings were press-fitted into 22.5 mm diameter holes drilled in the top and base acrylic plates to support and align the lead screw within the coating chamber. The sample holder supports were fabricated from 10 mm diameter hollow pipes to provide adequate rigidity while minimizing weight. Two crocodile clips, each mounted on a 100 mm long hollow pipe, were used as sample holders to allow secure gripping of samples and sufficient immersion depth during the coating process.

iii. Construction of the control system

The electronic components comprising the Arduino Uno microcontroller, A4988 stepper motor driver, capacitor, switch, keypad, potentiometer, and LCD screen was initially interconnected using jumper wires on a breadboard, as illustrated in Figure 2. This preliminary setup enabled verification of circuit functionality and ensured the accuracy of all electrical connections. After successful testing, the components were permanently mounted and soldered onto a circuit board. The assembled circuit was carefully inspected to eliminate solder bridges and ensure electrical reliability prior to integration with the mechanical system.

2.7.2 Assembly of the dip coater

Plate 1(a–d) illustrates the sequential stages involved in the assembly of the dip-coating machine. The mechanical components were assembled using M6 bolts and nuts, as shown in Plate 1(a) and (b). And to avoid vibration, the ends of the lead screw thread were accurately machine (no eccentricity) to fit into the bearings, the load on the carriage was balance on both sides. The screw shaft and the motor shaft were carefully aligned

Corresponding author's email address: send2mahmudmalik@yahoo.com

and connected using elastic coupling. The swivel that supported the coating chamber were place on elastic base. The frame was made sturdy and the fasteners were well tightened. The electronic control unit, which governs the motion of the dip-coating mechanism, was housed in a perforated polyethylene enclosure with dimensions of 155 mm × 150 mm × 75 mm (Plate 1(c)). The perforations on the enclosure walls facilitate adequate ventilation and prevent overheating of the electronic components. The user interface elements including the keypad, speed-control potentiometer, and LCD screen were mounted on the cover of the control box for ease of operation and visibility. Finally, the mechanical and electronic subsystems were integrated, as depicted in Plate 1(d). The assembled dip coater was subsequently calibrated to ensure compliance with the specified operational parameters required for the coating process.

2.8 Cost Estimate of the Assembled Dip Coater

The cost of the components used in the construction of the dip-coating system is summarized in Table 1. The total cost, including both mechanical and electrical components, amounted to ₦142,000, which is equivalent to USD 97.3 at the prevailing exchange rate of ₦1450/USD. This relatively low cost demonstrates the economic viability of the developed dip coater and highlights its suitability for laboratory-scale and low-budget research applications.

Table 1: Bill of Materials and Cost

Components/materials	Quantity/ Dimensions	Cost per unit (N)	Cost (N)
Angle sections	25mm × 25mm × 3mm by 1300mm	7,000	1,800
Screw rod	Ø10 × 50mm	2,000	1,000
PLA carriage	70mm × 90mm × 20mm	10,000	10,000
M6 bolts	24	20	500
Hollow steel pipe	Ø8 × 750mm	3,000	1,500
Swilve support	4	200	800
Hinge	2	200	400
Crocodile clip	2	500	1000
Perspex	1000mm × 700mm × 5mm		40,000
Roller/thrust bearings	4	1,500	6,000
Clip	2	100	200
Electronic Components			
NEMA 17 stepper motor (17HS440)	1	13,000	13,000
Motor driver (DRV8825)	1	4,500	4,500
Arduino microcontroller	1	20,000	20,000
DC power adaptor	1	15,000	15,000
Switch	1	500	500
Potentiometer	1	3,000	3,000
LCD display screen	1	4,000	4,000
4 by 4 matrix key pad	1	2,000	2,000
Circuit board	1	16,000	16,000
Voltage regulator	1	600	600
Perforated box	1	1,000	1,000
Total			142,000

2.9 Calibration and Uncertainty Analysis

Calibration of the dip-coating machine was carried out to ensure accurate correspondence between the programmed input parameters and the actual mechanical response of the system. The desired immersion height was converted into stepper motor motion using the relationship between the number of motor steps, the screw rod pitch, and the number of steps per revolution, as expressed in Equation (17) as given by Guzmán-valdivia *et al.,* (2025).

$$Number\ of\ steps = NSPR \times \frac{I_H}{SRP} \quad 17$$

Corresponding author's email address: send2mahmudmalik@yahoo.com

where NSPR is the number of steps per revolution, I_H is the inputted immersion height (mm), and SRP is the screw rod pitch (mm).

Experimental tests were conducted at immersion heights of 40, 60, 80, 100, and 120 mm according to the method of Loza *et al*, (2015), with each measurement repeated five times to obtain mean values. Any discrepancies between the programmed and measured immersion heights were corrected by introducing a calibration factor into Equation (17).

The immersion and withdrawal speeds were controlled by adjusting the pulse frequency supplied to the stepper motor (Rahman *et al*., 2025). The linear speed of the carriage is related to the motor step count, screw pitch, and pulse frequency, as given by Equation (18) (Castillo-Vilcatoma *et al.,* 2022):

$$speed\ in\ (\frac{mm}{s}) = \left[\frac{number\ of\ steps \times pitch\ distance\ per\ rev}{NSPR}\right] \times pulse\ frequency \quad 18$$

Pulse frequency was manually regulated using a potentiometer with a digital range of 0–1023 counts. Calibration of the pulse rates was performed based on the calibrated number of steps per immersion height to achieve the desired speed range. The potentiometer was graduated base on the desired speed range in a step of 1mm/s using the speed (rpm) readings from a tachometer and Equation (19).

$$graduation\ position\ in\ (\frac{mm}{s})(1-7) = \frac{N_{1-7} \times 60}{pitch\ distance\ per\ revolution} \quad 19$$

Uncertainty in the system originates from mechanical tolerances such as backlash in the screw rod–nut assembly and minor carriage misalignment, as well as electrical factors including pulse timing variability and the finite resolution of the potentiometer. Measurement uncertainty was reduced by repeated trials, and repeatability was assessed using the standard deviation of the measurements. Following calibration, the residual deviations between intended and measured immersion heights and speeds were within acceptable limits for laboratory-scale dip-coating applications, confirming the accuracy and repeatability of the developed system.

3. Results and Discussion

3.1 Calibration of the Dip-Coating Machine

After assembly, the dip-coating machine was operated and calibrated to evaluate its positional accuracy and speed control performance. Five repeated measurements were taken at different programmed immersion heights (40, 60, 80, 100, and 120 mm). The actual immersion heights were measured using a Vernier caliper, and the results are presented in Table 2.

Table 2: Measurement from Trial Operation of the Dip Coating Machine

S/No	Immersion height (input) (mm)	Immersion height (output) (mm)					Average	Error %
		Number of trials						
		1	2	3	4	5		
1	40	39.86	39.86	39.86	39.86	39.86	39.86	-0.35
2	60	59.79	59.80	59.79	59.79	59.80	59.80	-0.34
3	80	79.72	79.72	79.72	79.72	79.72	79.72	-0.35
4	100	99.65	99.66	99.66	99.65	99.65	99.66	-0.35
5	120	119.58	119.58	119.58	119.58	119.58	119.58	-0.35

The results in Table 2 show that the actual immersion heights were consistently slightly lower than the programmed input values. This systematic deviation is attributed primarily to a minor inclination of the dipping mechanism from the true vertical axis. Despite this offset, the machine exhibited high repeatability, as evidenced by the negligible variation among repeated measurements at each set point. To compensate for this systematic error, a correction factor of 1.000333, derived from the measured inclination angle, was incorporated into Equation (16). The calibrated immersion height results are presented in Table 3. The calibration procedure effectively eliminated the discrepancy between the input and output immersion heights, thereby significantly improving the positional accuracy of the dip-coating machine. This level of accuracy is essential for achieving uniform and reproducible coatings.

Corresponding author's email address: send2mahmudmalik@yahoo.com

Table 3 Comparison Between Initial and Calibrated Immersion Heights

S/No	Input	Output	
	Immersion height (mm)	Immersion height Before calibration (mm)	Immersion height after calibration (mm)
1	40	39.98	40.00
2	60	59.80	60.00
3	80	79.72	80.00
4	100	99.66	100.00
5	120	119.58	120.00

3.2 Speed Calibration and Control

The linear speed of the machine was evaluated at a maximum operating voltage of 9V and a limiting current of 5A. Under these conditions, the maximum attainable withdrawal speed was measured to be 7.7mm/s, corresponding to a step rate of 981.95 pulses/s. Based on this result, the operational speed of the dip-coating machine was calibrated to be adjustable between 1 mm/s and 7 mm/s in increments of 1 mm/s. Speed measurements were carried out using an EXTECH 461995 laser/contact tachometer, and the corresponding speed in mm/s were determined using Equation (19). The angular positions of the potentiometer corresponding to each speed increment were recorded and permanently marked on the potentiometer knob to facilitate repeatable speed selection. The graduated speed results are presented in Table 4.

Table 4.:Graduation of the Machine Speed

S/No	Graduation withdrawal speed (mm/s)	Expected withdrawal speed (rpm)	Measured Speed after graduation (rpm)	Measured Speed after graduation (mm/s)	Error (%)
1	1	40	39 ± 4	0.975	2.5
2	2	80	78 ± 5	1.95	2.5
3	3	120	120 ± 3	3.00	0
4	4	160	160 ± 4	4.00	0
5	5	200	202 ± 5	5.05	1.0
6	6	240	237 ± 3	5.925	1.25
7	7	280	280 ± 5	7	0

The speed calibration results demonstrate that the machine achieves accurate and stable speed control, with percentage errors generally below 2.5% consistent with accuracy reported by Yohandri *et al,* (2019). The use of a potentiometer with a digital resolution of 0–1023 counts enabled fine adjustment of pulse frequency, resulting in precise regulation of immersion and withdrawal speeds. Overall, the calibrated speed and positional control significantly enhance the reproducibility and accuracy of the dip-coating process, which is critical for achieving uniform coating thickness and consistent film quality across different samples.

4. Conclusion

A low-cost Arduino Uno microcontroller-based dip-coating machine for thin-film deposition was successfully developed using locally sourced and readily available components. The system performs controlled immersion, dwelling, and withdrawal operations with adjustable immersion height (70–220 mm from the base), speed (1–7 mm/s), and dwelling time (1–120 min), and was fabricated using basic manufacturing techniques. Calibration significantly improved system accuracy, reducing deviations between programmed and measured values from approximately 7.5% to less than 1%. The withdrawal mechanism demonstrated reliable and repeatable operation across the full speed range, ensuring consistent coating conditions. A key advantage of the developed system is its ability to simultaneously process multiple samples under identical operating parameters, thereby reducing experimental time during process optimization and scale-up studies. The total system cost remained below USD 100, making it a highly accessible and practical alternative to commercial dip coaters for academic and research laboratories, particularly in resource-limited environments. Future improvements may include the integration of real-time feedback control, a hot air source for accelerated solvent evaporation, and software-based data acquisition to further enhance system performance and experimental reproducibility.

Corresponding author's email address: send2mahmudmalik@yahoo.com

References

Adámek, P. 2016. Construction of dip-coater. Edukacja Technika Informatyka. 16(2):152–156. https://doi.org/10.15584/eti.2016.2.20.

Anwar, MA., Kurniawan, T., Asmara, YP., Harun, WSW., Oumar, AN. and Nandyanto, ABD. 2017. Morphology evaluation of ZrO_2 dip coating on mild steel and its corrosion performance in NaOH solution. IOP Conference Series: Materials Science and Engineering. 257(1): 012087.

Brinker, CJ. 2013. Dip coating: Chemical solution deposition of functional oxide thin films. in Chemical Solution Deposition of Functional Oxide Thin Films, Springer-Verlag Wien, Vienna. 233–261.

Castillo-Vilcatoma, DA., Loarte, SJ., Fernandez-Chillcce, AA., Pastrana, EC. and Pastrana, RY. 2021. Designing and fabrication of a low-cost dip-coater for rapid production of uniform thin films. Química Nova. XY(00):1–4. https://doi.org/10.21577/0100-4042.20170805.

Ceratti, DR., Louis, B., Paquez, X., Faustini, M. and Grosso, D. 2015. A new dip coating method to obtain large-surface coatings with a minimum of solution. Advanced Materials. 27(27):4037–4042.

Dunlap, C., Featherstone, S., Smith, M., Vu, M., Williams, A., Bailey, J. and Hu, H. 2022. Design and fabrication of a low-cost and programmable dip coating machine. HardwareX. 12:1–23.

Guzmán-Valdivia, CH., Azcaray-Rivera, HR., Martínez-Mata, AJ., Brizuela-Mendoza, JA., Buenabad-Arias, HM., Barrera-Sánchez, A., Blanco-Ortega, A. 2025. Design and validation of a low-cost automated dip-coater system for laboratory applications', Automation. 6(4):75. https://doi.org/10.3390/automation6040075.

Idris, RM., Yawas, DS. and Abdulrahman, AM., 2018. Development and performance evaluation of a three rollers acha (*Digitaria exilis*) dehusking machine. Arid Zone Journal of Engineering, Technology and Environment, 14(2),261-271.

Khurmi, RS. and Gupta, JK. 2005. Machine Design. New Delhi: Eurasia Publishing House (PVT) Ltd.

Loza, D., Guerrero, VH. and Dabirian, R. 2014. Construction of low-cost spin and dip coaters for thin film deposition using open source technology. Revista de Física. 49:13-25.

Nguyen-tri, P., Nguyen, TA. Carriere, P., Xuan, CN. 2018. Nanocomposite coatings: Preparation, characterization, properties, and applications. International Journal of Corrosion. 4749501. https://doi.org/10.1155/2018/4749501

Rahman, NR., Sya'roni, I., Hartanto, A., Prasetyono, AD. and Subiantoro, I. 2025. Design and build a microcontroller-based dip-coater tool with an automatic calibration system. Indonesian Physical Review. 8(1): 48–61.

Serrano-Pérez, J., Reyes-Rojas, A., Meléndez, AG. 2023. Dip-coater revolver machine for layer processing on metallic substrates. PÄDI Boletín Científico de Ciencias Básicas e Ingenierías del ICBI. 11(5):109–116.

Tang, X., Yan, X. 2017. Dip-coating for fibrous materials: Mechanism, methods and applications. Journal of Sol-Gel Science and Technology. 81:378–404.

Yohandri, Y., Khairunnisa, R. and Zainul, R. 2019. Development of a digital dip coating system-based microcontroller. Eksakta Berkala Ilmiah Bidang MIPA. 20(2):62–69.

Corresponding author's email address: send2mahmudmalik@yahoo.com